Transient Resonance Raman and Density Functional Theory Investigation of 4-Methoxyphenylnitrenium and 4-Ethoxyphenylnitrenium Ions†

Pik Ying Chan, Shing Yau Ong, Peizhi Zhu, Cunyuan Zhao, and David Lee Phillips*

Department of Chemistry, The University of Hong Kong, Pokfulam Road, Hong Kong S.A.R., P. R. China

Received: November 13, 2002; In Final Form: February 25, 2003

This paper presents a transient resonance Raman and density functional theory study of 4-methoxyphenylnitrenium and 4-ethoxyphenylnitrenium ions in a largely aqueous environment. The transient Raman bands observed in conjunction with the (U)BPW91/cc-PVDZ calculation results indicates these nitrenium ions are singlet state species. Both the 4-methoxyphenylnitrenium and the 4-ethoxyphenylnitrenium ions have significant iminocyclohexadienyl character to a degree very similar to that previously found for the 2-fluorenylnitrenium ion. The 4-methoxyphenylnitrenium and the 4-ethoxyphenylnitrenium ions also have significant oxocarbocation character and this influences both their properties and chemical reactivity. We compare the properties of the 4-methoxyphenylnitrenium and the 4-ethoxyphenylnitrenium ions to those previously found for other arylnitrenium ions.

Introduction

Arylnitrenium ions are believed to be key intermediates in chemical carcinogenesis and there has been a great deal of interest in their properties and chemical reactions.[1−18] Aromatic amines (such as 2-acetyl-aminofluorene) can be enzymatically converted into sulfate esters of the analogous *N*-hydroxylamines. These types of sulfate esters in aqueous media will spontaneously form an arylnitrenium ion and a sulfate anion.[13,17] Arylnitrenium ions such as the 2-fluorenylnitrenium ion can be selectively trapped by guanine bases in DNA and form adducts. These types of reactions are thought to result in carcinogenic mutations.[8−10,14,18] Arylnitrenium ions are reactive short-lived species that are difficult to study. Several photochemical methods have been developed to enable laser spectroscopy techniques to be used to directly probe arylnitrenium ions in room-temperature solutions.[19−33] The lifetimes of arylnitrenium ions and their rate constants for reactions with other molecules have been measured using time-resolved transient absorption experiments.[19−27,29,30] Recently, time-resolved infrared (TRIR) absorption spectroscopy and time-resolved resonance Raman (TR^3) spectroscopy have been used to investigate the structure and properties of several arylnitrenium ions.[28,31−33] These studies showed that the arylnitrenium ions have significant iminocyclohexadienyl character to varying degrees depending on their structure and substituents.[28,31−33] Several alkoxyphenylnitrenium ions including 4-methoxyphenylnitrenium and 4-ethoxyphenylnitrenium ions have been examined using time-resolved transient absorption spectroscopy and found to have relatively long lifetimes on the order of a millisecond.[34,35] We note that the 4-ethoxyphenylnitrenium ion is of particular interest because it would be formed from the carcinogen phenacetin that had found use as an analegesic until it was banned for use.

In this paper, we report the first transient resonance Raman spectra for the 4-methoxyphenylnitrenium and the 4-ethoxyphenylnitrenium ions. The transient Raman spectra display a number of bands for both nitrenium ions in a largely aqueous solution at room temperature. These Raman bands have vibrational frequencies that agree noticeably better with the (U)BPW91/cc-PVDZ computed vibrational frequencies for the singlet state than the triplet state for the 4-methoxyphenylnitrenium and the 4-ethoxyphenylnitrenium ions. This and the relatively large singlet−triplet energy gap from the (U)BPW91/cc-PVDZ calculations indicates these nitrenium ions are singlet state species. Both 4-methoxyphenylnitrenium and the 4-ethoxyphenylnitrenium ions display significant iminocyclohexadienyl character. We compare the properties of the 4-methoxyphenylnitrenium and the 4-ethoxyphenylnitrenium ions to those previously found for other arylnitrenium ions characterized by time-resolved vibrational spectroscopy.

Experimental and Computational Section

4-Methoxyphenyl azide and 4-ethoxyphenyl azide were prepared following a previously reported method for the synthesis of azide compounds.[36,37] The 4-methoxyphenyl azide was prepared as follows. In a 200 mL round-bottom flask, 4-methoxyaniline (4.92 g, 40 mmol) was dissolved in water (10 mL) that contained concentrated HCl (20 mL). This solution was cooled to below 5 °C in an ice bath and diazotized with a solution of $NaNO_2$ (4.14 g, 60 mmol) with distilled water (10 mL). The mixture was stirred in an ice bath for 1 h. A solution of NaN_3 (5.2 g, 80 mmol) in water (30 mL) was added at 0 °C and stirred for 30 min. Then, the mixture was allowed to warm to room temperature and stirred for an additional hour. The resulting suspension of solid was filtered to isolate product (∼3.5 g). The 4-methoxyphenyl azide was characterized as follows: ^{1}H NMR (400 MHz, CD_3CN): δ 7.01 (d, $J = 8.9$ Hz, 2H), δ 6.94 (d, $J = 8.9$ Hz, 2H), δ 3.77 (s, 3H): IR (film): 2106 cm^{-1}: MS (EI): *m*/*z*: 149 [$C_7H_7N_3O^+$], 121 [$C_7H_7NO^+$]; UV (CH_3CN): λ max = 256 nm.

4-Ethoxyphenyl azide was prepared as follows. In a 200 mL round-bottom flask, 4-ethoxyaniline (5.15 mL, 40 mmol) was dissolved in water (10 mL) that contained concentrated HCl (20 mL). This solution was cooled to below 5 °C in an ice bath and diazotized with a solution of $NaNO_2$ (4.14 g, 60 mmol)

† Part of the special issue "A. C. Albrecht Memorial Issue".

* To whom correspondence should be addressed. E-mail: phillips@hkucc.hku.hk. Fax: 852-2857-1586.

10.1021/jp0224261 CCC: $25.00
Published on Web 04/17/2003

with distilled water (10 mL). The mixture was stirred in an ice bath for 1 h. A solution of NaN_3 (5.2 g, 80 mmol) in water (30 mL) was added at 0 °C and stirred for 30min. Then, the mixture was allowed to warm to room temperature and stirred for an additional hour. Anhydrous potassium hydrocarbonate is added to neutralize the mixture. The product is then extracted by diethyl ether (~ 3 mL) and characterized as follows: ^{1}H NMR (400 MHz, CD_3CN): δ 6.97 (d, J = 9.1 Hz, 2H), δ 6.90 (d, J = 9.1 Hz, 2H), δ 3.99 (q, J = 7.0 Hz, 2H), δ 1.34 (t, J = 7.0 Hz, 3H): IR (liquid): 2109 cm^{-1}: MS (EI): *m*/*z*: 163 [$C_8H_9N_3O^+$], 135 [$C_8H_9NO^+$]; UV (CH_3CN): λ max = 256 nm.

Samples of the precursor compound (4-methoxyphenyl azide or 4-ethoxyphenyl azide) were prepared with concentrations of about 2.5 mM in a 60% water/40% acetonitrile mixed solvent by volume with an acetate buffer (2 mM) and a pH of 3.5. The transient resonance Raman spectra were obtained using an experimental apparatus and methods detailed previously so only a brief description will be presented here.[32,33,38] The harmonics of a pulsed Nd:YAG laser and their hydrogen Raman shifted laser lines were used for the pump (266 nm) and probe (320 nm) excitation wavelengths in the transient Raman experiments. An optical time-delay of approximately 10 ns between the pump and probe pulses was used in the experiments. The pump and probe laser beams were loosely focused onto a flowing liquid stream of sample using a near collinear and backscattering geometry. The Raman light was collected using reflective optics and imaged through a depolarizer and entrance slit of a 0.5 m spectrograph equipped with a liquid-nitrogen-cooled CCD. The grating of the spectrograph dispersed the Raman light onto the CCD that accumulated signal for about 300−600 s before being readout to an interfaced PC computer. Approximately 10−20 of these readouts were summed to obtain a spectrum. Pump only, probe only, and pump−probe spectra were acquired. A background scan was also obtained. The known Raman bands of the water/acetonitrile solvent were employed to calibrate the Raman shifts of the spectra. Subtraction of a probe only spectrum from the pump−probe spectrum was done to remove solvent and precursor Raman bands, and then the pump-only spectrum and background scan were also subtracted to finally obtain the transient Raman spectrum.

All of the density functional theory calculations presented here made use of the Gaussian 98W program suite[39] Complete geometry optimization and vibrational frequency computations were done analytically using the (U)BPW91 method[40,41] and the cc-PVDZ basis set.[42] Density functional theory (DFT) calculations at random-phase approximation[43] (RPA) were done to estimate the electronic transition energies and oscillator strengths for the 4-methoxyphenylnitrenium and 4-ethoxyphenylnitrenium ions.

Results and Discussion

Flash photolysis of alkoxyphenyl azides in a largely aqueous environment gives rise to strong transient absorption bands with maxima around 290−305 nm on the ns to ms time scale.[34,35] These transient absorption bands are attributed to alkoxyphenylnitrenium ions and are noticeably different than other arylnitrenium ions such as 4-biphenylylnitrenium and 2-fluorenylnitrenium ions that have transient absorption bands with maxima in the 430−460 nm region.[20,21,23−25,29] The 320 nm probe wavelength used in the transient resonance Raman experiments was chosen to be resonant with the red side of the transient absorption bands attributed to the 4-methoxyphenylnitrenium and 4-ethoxyphenylnitrenium ions. Figure 1 presents a typical pump only spectrum in the probe wavelength region (A), a probe only Raman spectrum (B), a pump−probe Raman spectrum (C), and a transient Raman spectrum (D) obtained by subtraction of probe only and pump only spectra from the pump−probe spectrum. The spectra in Figure 1 were obtained after 266 nm photolysis of 4-methoxyphenyl azide in 60% water/40% acetonitrile solvent (by volume). Figure 2 presents an expanded view of the transient resonance Raman spectrum due to 4-methoxyphenylnitrenium ion shown in Figure 1. Figure 3 presents the transient resonance Raman spectrum obtained for the 4-ethoxyphenylnitrenium ion obtained under similar conditions as the 4-methoxyphenylnitrenium ion in Figures 1 and 2. Comparison of experimental vibrational frequencies to those predicted from density functional theory (DFT) or ab initio calculations for

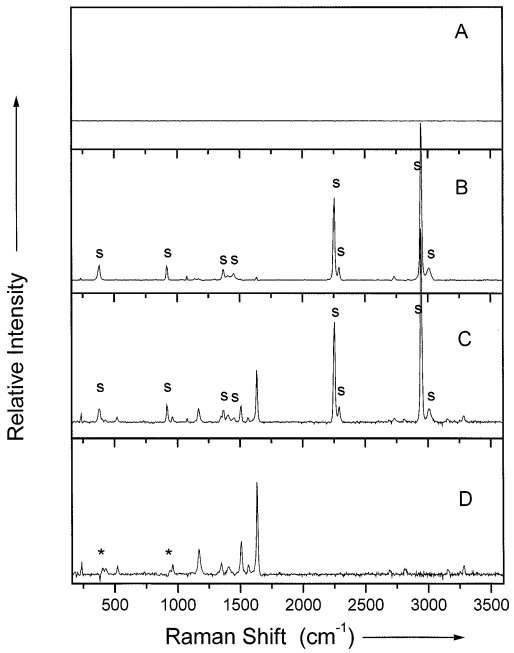

Figure 1. Examples of a typical 266 nm pump only spectrum in the probe wavelength region (A), a 320 nm probe only Raman spectrum (B), a pump−probe spectrum (C), and the resulting transient resonance Raman spectrum (D) of the 4-methoxyphenylnitrenium ion. "S" mark solvent bands (in B and C), whereas the asterisks mark solvent subtraction artifacts in the transient spectrum (D).

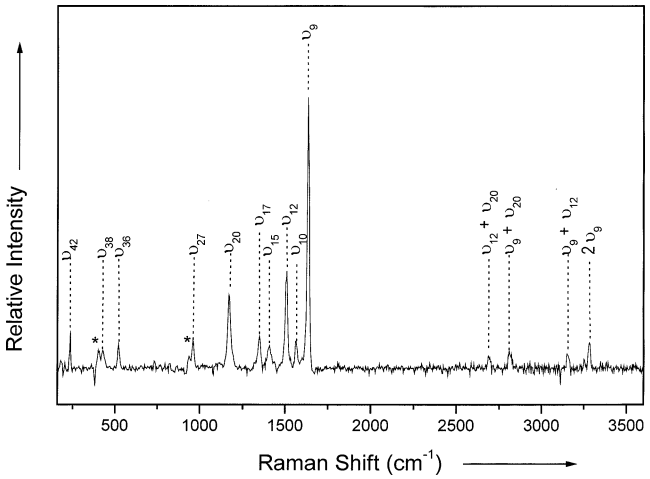

Figure 2. Expanded view of the transient resonance Raman spectrum of the 4-methoxyphenylnitrenium ion obtained using a 320 nm probe and 266 nm pump excitation wavelengths. The assignments of the larger Raman bands are labeled (see text and Table 1 for more details). The asterisks mark solvent subtraction artifacts.

TABLE 1: Experimental Raman Vibrational Frequencies Observed in the Time-Resolved Resonance Raman Spectra of the 4-Methoxyphenylnitrenium Ion Shown in Figure 2[a]

triplet 4-methoxyphenylnitrenium ion		singlet 4-methoxyphenylnitrenium ion		experiment
vibrational mode, possible description	UBPW91 cc-PVDZ calc. value (in cm^{-1})	vibrational mode, possible description	BPW91 cc-PVDZ calc. value (in cm^{-1})	10 ns time-resolved Raman freq. shift (in cm^{-1})
ν_{45}, ring def.	89	ν_{45}, ring def.	80	
ν_{44}, ring def.	156	ν_{44}, ring def.	154	
ν_{43}, CH_3 bend	175	ν_{43}, CH_3 bend	167	
ν_{42}, C−O bend	213	**ν_{42}, C−O bend**	**220**	**235**
ν_{41}, N−H bend	305	ν_{41}, C−O bend + C−N bend	273	
ν_{40}, N−H bend	317	ν_{40}, ring def. + N−H bend	349	
ν_{39}, ring def.	370	ν_{39}, C−N bend	381	
ν_{38}, CCC bend	403	**ν_{38}, CCC bend**	**413**	**428**
ν_{37}, N−H bend	453	**ν_{37}, C−H bend**	**510?**	
ν_{36}, ring def. + N−H bend	494	**ν_{36}, CCC bend**	**513**	**521**
ν_{35}, CCC bend + C−O−C bend	510	ν_{35}, ring def.	594	
ν_{34}, CCC bend	594	ν_{34}, ring def.	732	
ν_{33}, ring def. + N−H bend	676	ν_{33}, C−H bend + N−H bend	736	
ν_{32}, CCC bend	724	ν_{32}, ring def.	759	
ν_{31}, C−H bend	768	ν_{31}, ring def.	798	
ν_{30}, N−H bend + C−H bend	790	ν_{30}, C−H bend + N−H bend	856	
ν_{29}, ring def.	821	ν_{29}, C−H bend + N−H bend	890	
ν_{28}, N−H bend + C−H bend	849	**ν_{28}, ring def.**	**939**?	
ν_{27}, C−H bend	939	**ν_{27}, ring def.**	**946**	**960**
ν_{26}, C−H bend	952	ν_{26}, C−H bend + N−H bend	983	
ν_{25}, ring def. + N−H bend	956	ν_{25}, C−H bend	988	
ν_{24}, C−O stretch + N−H bend	965	ν_{24}, C−H bend + N−H bend	1069	
ν_{23}, CH_3 bend	1096	ν_{23}, CH_3 bend	1097	
ν_{22}, C−H bend	1098	ν_{22}, N−H bend + C−H bend	1135	
ν_{21}, CH_3 bend + C−H bend	1148	**ν_{21}, C−H bend**	**1146**?	
ν_{20}, C−H bend	1155	**ν_{20}, C−H bend+N−H bend+CH_3 bend**	**1150?**	**1169**
ν_{19}, C−H bend	1240	ν_{19}, C−H bend + N−H bend	1271	
ν_{18}, C−C str.	1284	ν_{18}, C−H bend + CH_3 bend	1316	
ν_{17}, C−H bend + CH_3 bend	1302	**ν_{17}, N−H and C−H bend**	**1374**	**1350**
ν_{16}, C−N str. + C−O str.	1351	**ν_{16}, C−H bend + N−H bend**	**1382**	
ν_{15}, CH_3 bend	1393	**ν_{15}, CH_3 bend**	**1413**	**1408**
ν_{14}, CH_3 bend	1416	**ν_{14}, CH_3 bend**	**1424?**	
ν_{13}, CH_3 bend	1422	ν_{13}, C−C str.	1435	
ν_{12}, C−C str.	1440	**ν_{12}, C−O str. + CH_3 bend**	**1485**	**1510**
ν_{11}, C−C str. + C−O str.	1467	ν_{11}, C−C str.	1549	
ν_{10}, C−C str.	1478	**ν_{10}, C−N str.**	**1571**	**1564**
ν_9, C−C str.	1606	**ν_9, C−C str.**	**1639**	**1632**
ν_8, C−H str.	2990	ν_8, C−H str.	3002	

[a] Possible vibrational band assignments are also shown based on comparison to calculated vibrational frequencies from UBPW91/cc-PVDZ or BPW91/cc-PVDZ computations in the 200 to 1700 cm^{-1} fingerprint region for the ground singlet and triplet state of 4-methoxyphenylnitrenium ion(see text). The experimental vibrational frequencies are compared to those from (U)BPW91/cc-PVDZ computations for the singlet and triplet sates of the 4-methoxyphenylnitrenium ion. See text for more details

probable photoproduct species has been used successfully to identify and assign time-resolved infrared (TRIR) and time-resolved resonance Raman (TR^3) spectra to arylnitrenium ions, arylnitrenes, and arylnitrene photoproducts.[28,31−33,38] A similar methodology will be used to assign the TR^3 spectra observed in Figures 1−3. We note that the lifetimes of arylnitrenium ions measured previously by transient absorption or TRIR experiments showed no discernible difference when done in O_2- and N_2-purged solutions.[31,35] Thus, we do not expect that removal of O_2 is likely to make any difference in the observed transient Raman spectra shown in Figures 1−3.

(U)BPW91/cc-PVDZ calculations were performed for the singlet and triplet states of the 4-methoxyphenylnitrenium and 4-ethoxyphenylnitrenium ions to find their total energy, optimized geometry, and vibrational frequencies. Tables 1 and 2 compare the experimental transient resonance Raman vibrational frequencies observed in Figures 2 and 3 to those predicted from the DFT calculations for the singlet and triplet states of the 4-methoxyphenylnitrenium and 4-ethoxyphenylnitrenium ions, respectively. Figure 4 presents simple schematic diagrams of the singlet and triplet states of the 4-methoxyphenylnitrenium

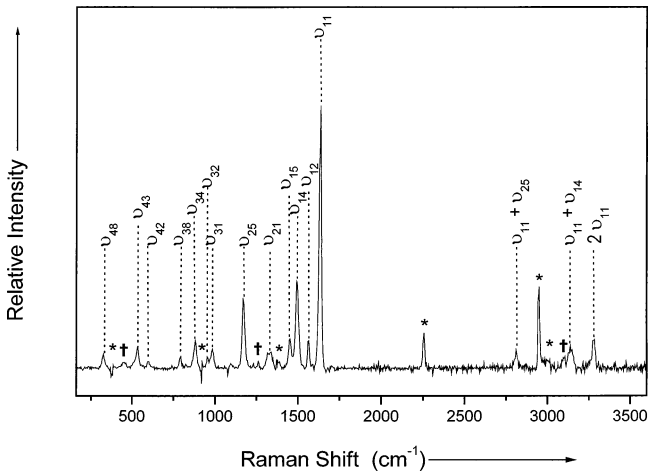

Figure 3. Expanded view of the transient resonance Raman spectrum of the 4-ethoxyphenylnitrenium ion obtained using a 320 nm probe and 266 nm pump excitation wavelengths. The assignments of the larger Raman bands are labeled (see text and Table 2 for more details). The asterisks mark solvent subtraction artifacts, and the daggers label small stray light or ambient light artifacts.

TABLE 2: Experimental Raman Vibrational Frequencies Observed in the Time-Resolved Resonance Raman Spectra of the 4-Ethoxyphenylnitrenium Ion Shown in Figure 3[a]

triplet 4-ethoxyphenylnitrenium ion		singlet 4-ethoxyphenylnitrenium ion		experiment
vibrational mode, possible description	UBPW91/cc-PVDZ calc. value (in cm^{-1})	vibrational mode, possible description	BPW91/cc-PVDZ calc. value (in cm^{-1})	10 ns time-resolved Raman freq. shift (in cm^{-1})
ν_{48}, C−O−C bend	308	**ν_{48}, CCC bend**	**304**	**326**
ν_{47}, N−H bend	314	ν_{47}, ring def. + N−H bend	350	
ν_{46}, ring def. + N−H bend	365	ν_{46}, C−N bend + C−O bend	369	
ν_{45}, N−H bend + C−O bend	412	ν_{45}, C−N bend	428	
ν_{44}, N−H bend	456	ν_{44}, C−H bend	508	
ν_{43}, C−H bend	495	**ν_{43}, CCC bend**	**523**	**532**
ν_{42}, CCC bend	524	**ν_{42}, ring def.**	**592**	**598**
ν_{41}, CCC bend	592	ν_{41}, C−H bend + N−H bend	730	
ν_{40}, ring def. + N−H bend	677	ν_{40}, C−O bend	731	
ν_{39}, C−O bend	734	ν_{39}, ring def.	761	
ν_{38}, C−H bend	766	**ν_{38}, ring def.**	**792**	**793**
ν_{37}, N−H bend + C−H bend	792	ν_{37}, C−H bend + CH_3 bend	794	
ν_{36}, C−H bend + CH_3 bend	796	ν_{36}, C−H bend	864	
ν_{35}, ring def.	816	ν_{35}, C−O str.	867	
ν_{34}, C−H bend + N−H bend	851	**ν_{34}, C−H bend + N−H bend**	**884**	**881**
ν_{33}, ring def. + C−O str.	881	ν_{33}, ring def.	939	
ν_{32}, C−H bend	939	**ν_{32}, C−C str.**	**965**	**952**
ν_{31}, C−H bend	953	**ν_{31}, C−H bend + N−H bend**	**979**	**982**
ν_{30}, ring def.	957	ν_{30}, C−H bend	991	
ν_{29}, C−C str.	978	ν_{29}, C−H bend + N−H bend	1068	
ν_{28}, C−C str + C−H bend	1096	ν_{28}, C−C str.	1098	
ν_{27}, C−H bend	1102	ν_{27}, CH bend + CH_3 bend	1103	
ν_{26}, C−H bend + CH_3 bend	1103	ν_{26}, C−H bend + N−H bend	1136	
ν_{25}, C−H bend	1155	**ν_{25}, C−H bend + N−H bend**	**1151**	**1169**
ν_{24}, C−C str.	1240	ν_{24}, C−H bend + CH_3 bend	1248	
ν_{23}, C−H bend + CH_3 bend	1247	ν_{23}, C−H bend + N−H bend	1269	
ν_{22}, C−C str.	1280	ν_{22}, C−H bend + CH_2 bend	1305	
ν_{21}, C−H bend + CH_2 bend	1301	**ν_{21}, C−H bend+CH_2 bend+CH_3 bend**	**1346**	**1328**
ν_{20}, C−N str.+C−H bend+CH_3 bend	1333	**ν_{20}, CH_2 bend+CH_3 bend**	**1361?**	
ν_{19}, C−N str. + CH_3 bend	1355	ν_{19}, C−C str.+N−H bend	1376	
ν_{18}, C−N str.+C−H bend+CH_2 bend	1367	ν_{18}, CH_2 bend+CH_3 bend	1415	
ν_{17}, CH_3 bend	1416	ν_{17}, CH_2 bend	1417	
ν_{16}, C−H bend	1418	**ν_{16}, C−C str. + CH_3 bend**	**1432**	**1452**
ν_{15}, C−C str. + CH_3 bend	1433	**ν_{15}, C−C str. + CH_3 bend**	**1436?**	
ν_{14}, C−C str. + CH_3 bend	1440	**ν_{14}, C−O str. + C−N str.**	**1469**	**1492**
ν_{13}, C−C str.	1459	ν_{13}, C−C str.	1553	
ν_{12}, C−C str.	1479	**ν_{12}, C−N str.**	**1572**	**1564**
ν_{11}, C−C str.	1605	**ν_{11}, C−C str.**	**1640**	**1636**
ν_{10}, C−H str.	2981	ν_{10}, C−H str.	2996	

[a] Possible vibrational band assignments are also shown based on comparison to calculated vibrational frequencies from UBPW91/cc-PVDZ or BPW91/cc-PVDZ computations in the 200 to 1700 cm^{-1} fingerprint region for the ground singlet and triplet state of 4-ethoxyphenylnitrenium ion(see text). The experimental vibrational frequencies are compared to those from (U)BPW91/cc-PVDZ computations for the singlet and triplet sates of 4-ethoxyphenylnitrenium ion. See text for more details.

and 4-ethoxyphenylnitrenium ions with selected DFT optimized geometry bond lengths indicated next to the appropriate bonds. Inspection of Figure 4 shows that the singlet states of the 4-methoxyphenylnitrenium and 4-ethoxyphenylnitrenium ions have significantly more imine character (stronger C═N bonds) accompanied by more cyclohexadienyl (greater carbon−carbon bond length alternation) and oxo (stronger C═O bonds) character compared to their respective triplet states. These differences in structure lead to noticeable differences in the vibrational frequencies of the singlet and triplet states and enable them to be distinguished from one another using vibrational spectroscopy.

We note that there are circumstances where the ground state of the arylnitrenium ion may be a triplet state when a bulky aryl ligand or π-acceptor substituent may substantially destabilize the singlet state relative to the triplet state.[14,24] However, this is uncommon, and there are only a few reports that predict or observe triplet ground-state arylnitrenium ions.[14,24] The singlet−triplet gaps change as a function of substituents para to the nitrenium ion moiety and as the π-donating character of the subsituent increases the singlet state is more stabilized over the triplet state.[31,44] This leads to greater differences in the structures of the singlet and triplet states for stronger π-donating para substituents such as phenyl and alkoxy groups. We performed single-point energy calculations for the 4-methoxynitrenium and 4-ethoxynitrenium ions at the (U)BPW91/cc-PVDZ optimized geometry and found singlet−triplet gaps of 28.0 and 28.1 kcal/mol, respectively, at the (U)BPW91/cc-PVDZ level of theory and 35.1 and 35.5 kcal/mol, respectively, at the (U)MP2/cc-PVDZ level of theory with the singlet state being more stable in each case. This indicates the singlet states of the 4-methoxynitrenium and 4-ethoxynitrenium ions are substantially more stable than their triplet states. This and the fast formation of the nitrenium ions by protonation of the initially produced singlet arylnitrene precursor[35] suggests that the transient resonance Raman spectra observed in Figures 2 and 3 are due to the singlet state 4-methoxynitrenium and 4-ethoxynitrenium ions similar to the assignment of the transient absorption and resonance Raman spectra of the 2-fluorenylnitrenium ion to the singlet state.[19,22,32]

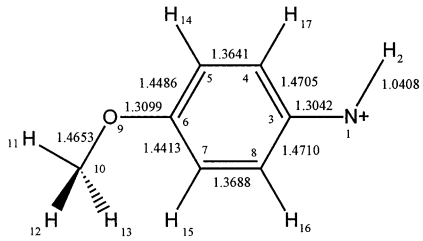

4-methoxyphenylnitrenium ion (Singlet)

where C4-C3-N1-H2 = 0.0
C7-C6-O9-C10 = 0.0

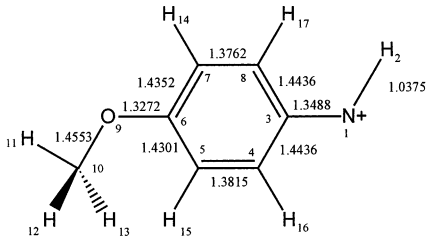

4-methoxyphenylnitrenium ion (Triplet)

where C8-C3-N1-H2 = 92.1
C5-C6-O9-C10 = -0.2

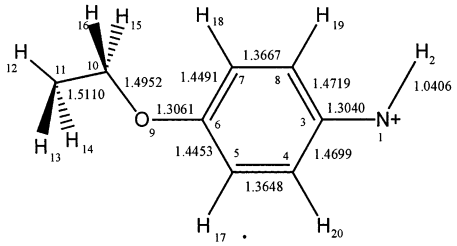

4-ethoxyphenylnitrenium ion (Singlet)

where C8-C3-N1-H2 = 0.0
C7-C6-O9-C10 = 0.0

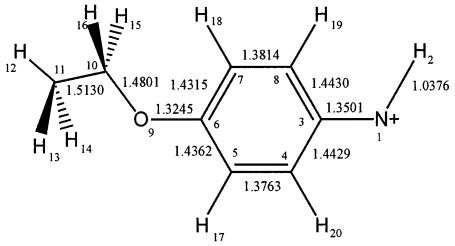

4-ethoxyphenylnitrenium ion (Triplet)

where C8-C3-N1-H2 = -94.1
C7-C6-O9-C10 = -0.3

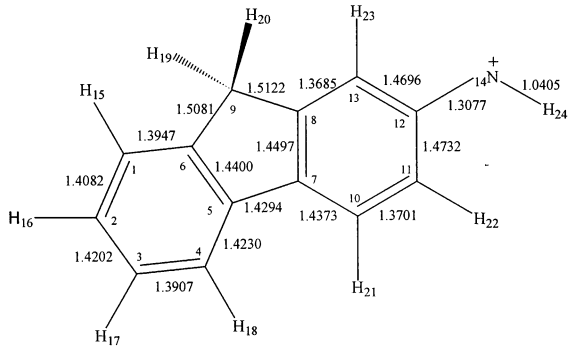

2-fluorenylnitrenim ion (singlet)

Figure 4. Diagrams of the singlet and triplet states of the 4-methoxyphenylnitrenium and 4-ethoxyphenylnitrenium ions with the atoms numbered. A diagram of the singlet state of the 2-fluorenylnitrenium ion is also given for comparison purposes. Selected bond lengths are shown (in Å) from the (U)BPW91/cc-PVDZ computations.

Inspection of Table 1 shows that the transient resonance Raman vibrational frequencies are in noticeably better agreement with the frequencies predicted for the singlet 4-methoxyphenylnitrenium ion than for the corresponding triplet state. The singlet state calculated vibrational frequencies are different from the experimental Raman frequencies by about 13.8 cm^{-1} on average compared to differences of about 24.3 cm^{-1} on average for the triplet state. Examination of Table 2 shows a similar agreement of the experimental Raman frequencies of Figure 3 to those predicted for the singlet state of 4-ethoxyphenylnitrenium ion (differences of about 11 cm^{-1} on average) compared to the corresponding triplet state (differences of about 16.5 cm^{-1} on average). Figure 5 compares the computed vibrational frequencies and relative Raman intensities for the singlet and triplet states of the 4-methoxyphenylnitrenium ion to the experimental resonance Raman spectrum vibrational frequencies and relative intensities. Inspection of Figure 5 shows that the experimental vibrational frequencies and relative Raman intensities exhibit a good correlation with those computed for the singlet 4-methoxyphenylnitrenium ion but not for the triplet state. This and the large computed singlet−triplet gap with the singlet state being more stable leads us to assign the transient Raman spectra in Figures 2 and 3 to the singlet states of 4-methoxyphenylnitrenium and 4-ethoxyphenylnitrenium ions, respectively.

Closer examination of Tables 1 and 2 and Figure 5 shows that the vibrational bands in the 1450−1650 cm^{-1} region are particularly useful to distinguish between the singlet and triplet states of these arylnitrenium ions. For example, in the 1450−1650 cm^{-1} region, the singlet state of the 4-methoxyphenylnitrenium ion has predicted vibrational bands at 1485, 1549, 1571, and 1639 cm^{-1}, whereas the triplet state has predicted bands at

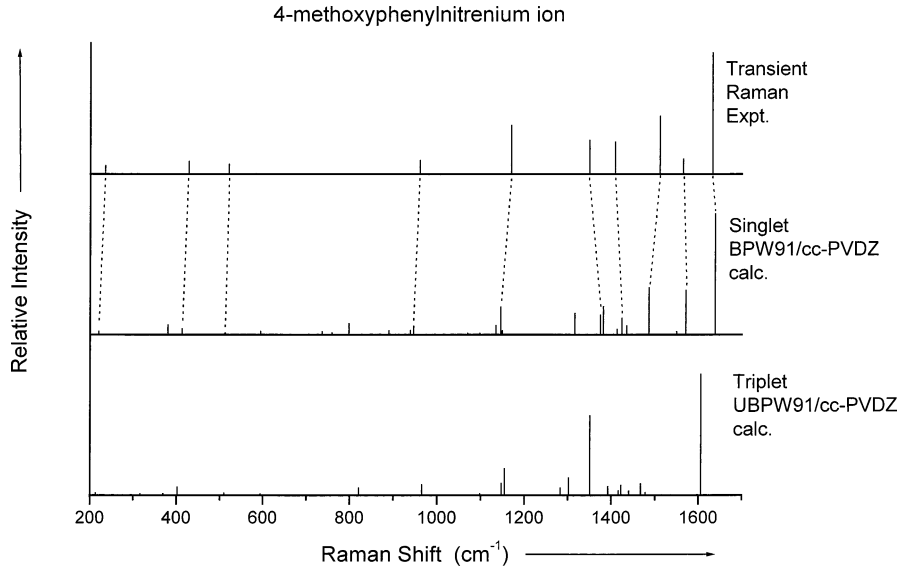

Figure 5. Comparison of the experimental transient Raman vibrational frequencies and relative intensities (from Figure 2) to those computed for the singlet and triplet states of the 4-methoxyphenylnitrenium ion. The largest Raman band in the 1600 cm^{-1} region is scaled to be 100 for all three diagrams. Only Raman bands with intensity >1 are shown. The dashed lines help indicate the correlation between the spectra.

TABLE 3: Electronic Transition Energies and Oscillator Strengths Obtained from RPA/cc-PVDZ Calculations Using the BPW91/cc-PVDZ Optimized Geometry for the Singlet 4-Methoxyphenylnitrenium and 4-Ethoxyphenylnitrenium Ions

species	singlet transition energies	oscillator strength
4-methoxyphenylnitrenium ion	566.6 nm	0.0006
	405.0 nm	0.0145
	320.7 nm	0.0000
	303.3 nm	**0.3327**
	260.1 nm	0.0003
	257.3 nm	0.0000
	236.5 nm	0.0095
	217.0 nm	0.0001
4-ethoxyphenylnitrenium ion	563.4 nm	0.0006
	410.4 nm	0.0244
	361.3 nm	0.0377
	338.2 nm	0.0001
	297.1 nm	0.0000
	292.6 nm	**0.3090**
	278.5 nm	0.0000
	256.8 nm	0.0000

1467, 1478, and 1605 cm^{-1}. The transient Raman frequencies observed at 1510, 1564, and 1633 cm^{-1} in the 1450−1650 cm^{-1} region in Figures 2 and 5 exhibit substantially better agreement with those computed for the singlet state (differences on average of 12.7 cm^{-1}) compared to the triplet state (differences of about 53 cm^{-1} on average) for these three modes. In addition, the relative intensity pattern for these vibrational modes are significantly different for the singlet and triplet states as seen in Figure 5. The vibrational modes in the 1450 to 1650 cm^{-1} region are sensitive and diagnostic of the degree of imine, cyclohexadienyl, and oxo character of the alkoxyphenylnitrenium ions.

We used density functional theory (DFT) computations at the random-phase approximation[43] (RPA) to estimate the electronic transition energies and oscillator strengths for the singlet state 4-methoxyphenylnitrenium and 4-ethoxyphenylnitrenium ions, and these results are presented in Table 3. Inspection of Table 3 reveals that the singlet state 4-methoxyphenylnitrenium and 4-ethoxyphenylnitrenium ions have only one large oscillator strength electronic transition at ∼303 and ∼292.6 nm respectively in the 200−1000 nm region. These results are consistent with experimental results that show these ions have strong transient absorption bands with maxima around 290−305 nm on the ns to ms time scale.[34,35] This is consistent with and provides further support for our assignment of the transient resonance Raman spectra shown in Figures 2 and 3 to the singlet states of the 4-methoxyphenylnitrenium and 4-ethoxyphenylnitrenium ions.

It is interesting to compare the structural properties of the singlet 4-methoxyphenyl nitrenium and 4-ethoxyphenylnitrenium ions to those of previously investigated arylnitrenium ions (note all structural comparisons discussed are made based on the same BPW91/cc-PVDZ level of calculated structures).[28,31−33] The imine character of the 4-methoxyphenyl nitrenium and 4-ethoxyphenylnitrenium ions is very strong (C═N bonds of about 1.3042 and 1.3040 Å respectively) and comparable to that of the 2-fluorenylnitrenium ion (with a C═N bond of about 1.3077 Å).[32,33] The C═N imine bonds in the 4-methoxyphenyl nitrenium, and 4-ethoxyphenylnitrenium ions are noticeably stronger than in the 4-biphenylylnitrenium ion (1.3083 Å),[33] diphenylnitrenium ion (1.3512 Å),[28,33] *N*-(4-biphenylyl)-*N*-methylnitrenium ion (1.321 Å),[31] *N*-(4-methylphenyl)-*N*-methylnitrenium ion (1.323 Å),[31] *N*-(4-chlorophenyl)-*N*-methylnitrenium ion (1.323 Å),[31] and *N*-(4-methoxyphenyl)-*N*-methylnitrenium ion (1.317 Å).[31] Similarly, the degree of C−C bond alternation (cyclohexadienyl character) in the phenyl ring to which the nitrenium moiety is attached is also very strong in the two 4-alkoxyphenylnitrenium ions examined and comparable to that found in the 2-fluorenylnitrenium ion.[32,33] For example, the first phenyl ring in the 2-fluorenylnitrenium ion has C12−C11 of 1.4732 Å; C11−C10 of 1.3701 Å; and C10−C7 of 1.4373 Å and C12−C13 of 1.4696 Å; C13−C8 of 1.3685 Å; and C8−C7 of 1.4497 Å (see Figure 4 for numbering system) compared to C3−C8 of 1.4710 Å; C8−C7 of 1.3688 Å; and C7−C6 of 1.4413 Å and C3−C4 of 1.4705 Å; C4−C5 of 1.3641 Å; and C5−C6 of 1.4486 Å for the singlet 4-methoxyphenylnitrenium ion (see Figure 4). Our results clearly indicate that the alkoxyphenylnitrenium ions have a large degree of iminocyclohexadienyl character with an amount similar to the 2-fluorenylnitrenium ion. This is consistent with the similarity of the

experimental resonance Raman vibrational frequencies of the symmetric aromatic C═C stretch mode that is observed at 1633 cm^{-1} in the 4-methoxyphenylnitrenium ion and at 1636 cm^{-1} in the 4-ethoxyphenylnitrenium ion compared to 1633 or 1637 cm^{-1} in the 2-fluorenylnitrenium ion.[32,33] The symmetric aromatic C═C stretch vibrational mode in the 1568−1650 cm^{-1} region has previously been demonstrated to exhibit a good correlation with the degree of iminocyclohexadienyl character of a range of arylnitrenium ions,[28,31−33] and the alkoxynitrenium ions studied here also show this type of correlation.

The large degree of iminocyclohexadienyl character found in the 2-fluorenylnitrenium ion was largely attributed to the substitution of a second phenyl ring para to the nitrenium ion and the tendency of the biphenyl-like rings to go toward a more quinoidal-like structure as charge delocalized into the phenyl rings as well as the locking fluorene bridge that enhances this tendency.[32,33] However, the alkoxyphenylnitrenium ions do not have this second phenyl ring, and it is the alkoxy substitution para to the nitrenium ion moiety that appears to cause a similar effect as a para substituted phenyl group. Instead of charge delocalization proceeding through a quinoidal-like structure into two phenyl rings as in the 2-fluorenylnitrenium ion, the charge in the alkoxyphenylnitrenium ion tends to proceed to the C═O group leading to a significant charge on the C═O group and noticeable imine and oxo cyclohexadienyl character.

As the alkoxy group is changed from methoxy to ethoxy for the singlet alkoxyphenylnitrenium ions in Figure 4, the degree of imine and oxo character increase somewhat at the same time: the C═N bond decreases from 1.3042 to 1.3040 Å, and the C═O bond decreases from 1.3099 to 1.3061 Å. This imine and oxo character of the 4-alkoxyphenylnitrenium ions can also be affected by changing the character of the nitrenium moiety from $-NH^+$ to NCH_3^+. For example, the singlet 4-methoxyphenylnitrenium ion had C═N and C═O bond lengths of about 1.3042 and 1.3099 Å, respectively, that become weaker and lengthen to about 1.317 and 1.316 Å, respectively, in the *N*-(4-methoxyphenyl)-*N*-methylnitrenium ion (1.317 Å).[31] This lesser imine and oxo character is also accompanied by a smaller cyclohexadienyl character in *N*-(4-methoxyphenyl)-*N*-methylnitrenium ion[31] compared to the 4-methoxyphenylnitrenium ion. The nitrenium ion moiety charge delocalization into the phenyl ring of 4-alkoxyphenylnitrenium ions leads to greater oxo and imine character that is accompanied by cyclohexadienyl character. The charge that would be delocalized further into a second phenyl ring in systems such as the 2-fluorenylnitrenium ion[32] (or other para phenyl substituted arylnitrenium ions such as 4-biphenylylnitrenium ion[33] and N−(4-biphenylyl)-*N*-methylnitrenium ion[31]) mainly concentrates at the C═O group and gives the 4-alkoxyphenylnitrenium ions substantial oxocarbocation character. This has important implications for the properties and chemical reactivity of 4-alkoxyphenylnitrenium ions compared to para phenyl substituted arylnitrenium ions as discussed below.

The 4-alkoxyphenylnitrenium ions have been previously noted to have intriguing properties and chemical reactivity compared to para phenyl substituted arylnitrenium ions. For example, the 4-alkoxyphenylnitrenium ions have lifetimes similar to para phenyl substituted arylnitrenium ions such as the biphenyl-4-ylnitrenium ion[34,35,45] even though 4-alkoxy substitution is much more cation stabilizing on the σ^+ scale than the 4-phenyl substitution. In addition, it was found that adding another phenyl group between the methoxy moiety and the nitrenium ion moiety in the 4′-methoxybiphenyl-4-ylnitrenium ion gave an almost 3 orders of magnitude longer lifetime on the order of milliseconds.[29] McClelland and Ramlall[35] suggested that this could be due to the 4-alkoxyphenylnitrenium ions reacting like oxocarbocations and the greater charge delocalization in the biphenylyl systems leads to lower oxocarbocation character and a longer lifetime. Our present results showing that 4-alkoxyphenylnitenium ions have significant oxocarbocation character and combined with our previous work on para phenyl substituted arylnitrenium ions demonstrating effective charge delocalization into the para substituted phenyl ring[32,33] provide support for this hypothesis. The barriers to reaction with water for oxocarbocations have been suggested to be lower for those with greater charge on the oxocarbo moiety compared to those in which the charge is more delocalized.[46]

The oxocarbocation character of the 4-alkoxyphenylnitrenium ions also appears to influence the chemical reactivity of these ions toward nucleosides such as 2′deoxyguanosine. For example, the biphenyl-4-yl-nitrenium and the 4′-methoxybiphenyl-4-ylnitrenium ions exhibited significant selectivity toward reaction with 2′-deoxyguanosine even in the nucleophilic solvent water,[30] whereas this selectivity was not found for the 4-alkoxyphenylnitrenium ions.[34,35] This was suggested to be due to greater charge at the oxocarbo group in the alkoxyphenylnitrenium ions and hence a lesser charge and reactivity at the nitrenium moiety.[35] Our present results are reasonably consistent with this hypothesis in that there does appear to be a noticeable localization of charge at the oxocarbo moiety at the expense of the nitrenium ion moiety. However, the nitrenium moiety appears to have an imine character and charge very similar to that found in the 2-fluorenylnitrenium and 4-biphenylylnitenium ions. Thus, we speculate that the different chemical reactivity of the alkoxynitrenium ions toward nucleosides such as 2′-deoxyguanosine is not just an effect of charge localization and is also due to an increase in chemical reactivity toward nucleosides such as water (via the oxocarbocation site). This could lead to a situation where reaction with water (via the oxocarbocation site) has a rate relative to the reaction of the nitrenium ion moiety with nucleosides such as 2′-deoxyguanosine so that the overall alkoxynitrenium ion exhibits little selectivity toward 2′-deoxyguanosine as found in previous laser flash studies.[34,35] This hypothesis would also be consistent with the 4′-methoxybiphenyl-4-ylnitrenium ion exhibiting some selectivity toward 2′-deoxyguanosine because this arylnitrenium ion would have significantly less charge on the methoxy group (so its oxocarbocation character and reactivity would be significantly less than in the 4-alkoxyphenylnitrenium ions), whereas the nitrenium ion moiety would still retain a reactivity like the 4-biphenylylnitrenium ion. Further work is needed to see if this is actually the case. Additional studies of the chemical reactions of alkoxyarylnitrenium ions using a variety of experimental techniques should prove useful to more fully understand the chemical behavior of these interesting arylnitrenium ions.

Acknowledgment. This work was supported by grants from the Committee on Research and Conference Grants (CRCG), the Research Grants Council (RGC) of Hong Kong (HKU 7112/00P), and the Large Items of Equipment Allocation 1993−94 from the University of Hong Kong.

Supporting Information Available: The Cartesian coordinates, energies, zero-point energy corrections, and predicted vibrational frequencies and intensities from the (U)BPW91/cc-PVDZ density functional theory calculations are given for the singlet and triplet states of the 4-methoxyphenylnitrenium and 4-ethoxyphenylnitrenium ions. Single-point energy calculations are also given for the singlet and triplet states of the 4-meth-

oxyphenylnitrenium and 4-ethoxyphenylnitrenium ions at the (U)BPW91/cc-PVDZ and (U) MP2/cc-PVDZ levels of theory using the (U)BPW91/cc-PVDZ optimized geometry. This material is available free of charge via the Internet at http://pubs.acs.org.

References and Notes

(1) Miller, J. A. *Cancer Res.* **1970**, *20*, 559.
(2) Scribner, J. D.; Naimy, N. K. *Cancer Res.* **1975**, *35*, 1416.
(3) Miller, E. C. *Cancer Res.* **1978**, *38*, 1479.
(4) Miller, E. C.; Miller, J. A. *Cancer* **1981**, *47*, 2327.
(5) Singer, B.; Kusmierek, J. T. *Annu. Rev. Biochem.* **1982**, *51*, 655.
(6) Miller, J. A.; Miller, E. C. *Environ. Health Perspect.* **1983**, *49*, 3.
(7) Garner, R. C.; Martin, C. N.; Clayson, D. B. In *Chemical Carcinogens*, 2nd ed.; Searle, C. E., Ed.; ACS Monograph 182; American Chemical Society: Washington DC, 1984; Vol. 1, pp 175−276.
(8) Famulok, M.; Boche, G. *Angew. Chem., Int. Ed. Engl.* **1989**, *28*, 468.
(9) Meier, C.; Boche, G. *Tetrahedron Lett.* **1990**, *31*, 1693.
(10) Humphreys, W. G.; Kadlubar, K. K.; Guengerich, F. P. *Proc. Natl. Acad. Sci. U.S.A.* **1992**, *89*, 8278.
(11) Kadlubar, F. F. In *DNA Adducts of Carcinogenic Amines*; Hemminiki, K., Dipple, A., Shuker, D. E. G., Kadlubar, K. K., Segerbäch, D., Bartsch, H., Ed.; Oxford University Press: Oxford, U.K., 1994; pp 199−216.
(12) Dipple, A. *Carcinogenesis* **1995**, *16*, 437.
(13) Novak, M.; Kahley, M. J.; Lin, J.; Kennedy, S. A.; James, T. G. *J. Org. Chem.* **1995**, *60*, 8294.
(14) Cramer, C. J.; Falvey, D. E. *Tetrahedron Lett.* **1997**, *38*, 1515.
(15) Novak, M.; Kennedy, S. A. *J. Am. Chem. Soc.* **1995**, *117*, 574.
(16) Hoffman, G. R.; Fuchs, R. P. P. *Chem. Res. Toxicol.* **1997**, *10*, 347.
(17) Novak, M.; Kennedy, S. A. *J. Phys. Org. Chem.* **1998**, *11*, 71.
(18) Novak, M.; VandeWater, A. J.; Brown, A. J.; Sanzebacher, S. A.; Hunt, L. A.; Kolb, B. A.; Brooks, M. E. *J. Org. Chem.* **1999**, *64*, 6023.
(19) McClelland, R. A.; Ahmad, A.; Dicks, A. P.; Licence, V. *J. Am. Chem. Soc.* **1999**, *121*, 3303.
(20) Anderson, G. B.; Falvey, D. E. *J. Am. Chem. Soc.* **1993**, *115*, 9870.
(21) Davidse, P. A.; Kahley, M. J.; McClelland, R. A.; Novak, M. *J. Am. Chem. Soc.* **1994**, *116*, 4513.
(22) McClelland, R. A.; Davidse, P. A.; Hadialic, G. *J. Am. Chem. Soc.* **1995**, *117*, 4173.
(23) Robbins, R. J.; Yang, L. L.-N.; Anderson, G. B.; Falvey, D. E. *J. Am. Chem. Soc.* **1995**, *117*, 6544.
(24) Srivastava, S.; Falvey, D. E. *J. Am. Chem. Soc.* **1995**, *117*, 10186.
(25) McClelland, R. A.; Kahley, M. J.; Davidse, P. A.; Hadzialic, G. *J. Am. Chem. Soc.* **1996**, *118*, 4794.
(26) Robbins, R. J.; Laman, D. M.; Falvey, D. E. *J. Am. Chem. Soc.* **1996**, *118*, 8127.
(27) Moran, R. J.; Falvey, D. E. *J. Am. Chem. Soc.* **1996**, *118*, 8965.
(28) Srivastava, S.; Toscano, J. P.; Moran, R. J.; Falvey, D. E. *J. Am. Chem. Soc.* **1997**, *119*, 11552.
(29) Ren, D.; McClelland, R. A. *Can. J. Chem.* **1998**, *76*, 78.
(30) McClelland, R. A.; Gadosy, T. A.; Ren, D. *Can. J. Chem.* **1998**, *76*, 1327.
(31) Srivastava, S.; Ruane, P. H.; Toscano, J. P.; Sullivan, M. B.; Cramer, C. H.; Chiapperino, D.; Reed, E. C.; Falvey, D. E. *J. Am. Chem. Soc.* **2000**, *122*, 8271.
(32) Zhu, P.; Ong, S. Y.; Chan, P. Y.; Leung, K. H.; Phillips, D. L. *J. Am. Chem. Soc.* **2001**, *123*, 2645.
(33) Zhu, P.; Ong, S. Y.; Chan, P. Y.; Poon, Y. F.; Leung, K. H.; Phillips, D. L. *Chem. Eur. J.* **2001**, *7*, 4928.
(34) Sukhai, P.; McClelland, R. A. *J. Chem. Soc., Perkin Trans. 2* **1996**, 1529.
(35) Ramlall, P.; McClelland, R. A. *J. Chem. Soc., Perkin Trans. 2* **1999**, 225.
(36) Brown, B. R.; Yielding, L. W.; White, W. E., Jr. *Mutat. Res.* **1980**, *70*, 17.
(37) White, W. E., Jr.; Yielding, L. W. In *Methods in Enzymology Vol. XLVI Affinity Labeling*; Jakoby, W. B., Wilchek, M., Eds.; Academic Press: Orlando, FL, 1977; pp 646−647.
(38) Ong, S. Y.; Zhu, P.; Poon, Y. F.; Leung, K. H.; Fang, W.-H.; Phillips, D. L. *Chem. Eur. J.* **2002**, *8*, 2163.
(39) Frisch, M. J.; Trucks, G. W.; Schlegel, H. B.; Scuseria, G. E.; Robb, M. A.; Cheeseman, J. R.; Zakrzewski, V. G.; Montgomery, J. A., Jr.; Stratmann, R. E.; Burant, J. C.; Dapprich, S.; Millam, J. M.; Daniels, A. D.; Kudin, K. N.; Strain, M. C.; Farkas, O.; Tomasi, J.; Barone, V.; Cossi, M.; Cammi, R.; Mennucci, B.; Pomelli, C.; Adamo, C.; Clifford, S.; Ochterski, J.; Petersson, G. A.; Ayala, P. Y.; Cui, Q.; Morokuma, K.; Malick, D. K.; Rabuck, A. D.; Raghavachari, K.; Foresman, J. B.; Cioslowski, J.; Ortiz, J. V.; Stefanov, B. B.; Liu, G.; Liashenko, A.; Piskorz, P.; Komaromi, I.; Gomperts, R.; Martin, R. L.; Fox, D. J.; Keith, T.; Al-Laham, M. A.; Peng, C. Y.; Nanayakkara, A.; Gonzalez, C.; Challacombe, M.; Gill, P. M. W.; Johnson, B. G.; Chen, W.; Wong, M. W.; Andres, J. L.; Head-Gordon, M.; Replogle, E. S.; Pople, J. A. *Gaussian 98*; Gaussian, Inc.: Pittsburgh, PA, 1998.
(40) Becke, A. *J. Chem. Phys.* **1986**, *84*, 4524.
(41) Perdew, J. P.; Burke, K.; Wang, Y. *Phys. Rev. B* **1996**, *54*, 16533.
(42) Dunning, T. H. *J. Chem. Phys.* **1989**, *90*, 1007.
(43) Bauernschmitt, R.; Ahlrichs, R. *Chem. Phys. Lett.* **1996**, *256*, 454.
(44) Sullivan, M. B.; Brown, K.; Cramer, C. J.; Truhlar, D. G. *J. Am. Chem. Soc.* **1998**, *120*, 11778.
(45) Novak, M.; Kahley, M. J.; Lin, J.; Kennedy, S. A.; Swanegan, L. A. *J. Am. Chem. Soc.* **1994**, *116*, 11626.
(46) Richard, J. P.; Amyes, T. L.; Jagannadham, V.; Lee, Y.-G.; Rice, D. J. *J. Am. Chem. Soc.*, **1995**, *117*, 5198.